

Issues of Microscopic Reversibility and an Isomeric Intermediate in Ligand Substitution Reactions of Five-Coordinate Oxorhenium(V) Dithiolate Complexes

David W. Lahti and James H. Espenson*

Contribution from the Ames Laboratory and Department of Chemistry, Iowa State University of Science and Technology, Ames, Iowa 50011

Received December 1, 2000. Revised Manuscript Received May 1, 2001

Abstract: Ligand substitution reactions between five-coordinate oxorhenium(V) dithiolates, $[\text{CH}_3\text{ReO}(\text{SCH}_2\text{C}_6\text{H}_4\text{S})\text{X}]$, or $\text{MeReO}(\text{mtp})\text{X}$, and entering ligands Y have been studied; Y is a phosphine and X is a phosphine (usually) or a pyridine. Many of them occur in two distinct stages, and other two-stage reactions merge to a single kinetic term when the successive rate constants are quite different in value. An intermediate can be detected directly by electronic and NMR spectroscopy. Just for phosphines, the range of rate constants is remarkably large; in the first stage, k spans the range 10^{-4} – 10^1 $\text{L mol}^{-1} \text{s}^{-1}$ at 25 °C in benzene; in the second, which also shows a first-order dependence on the concentration of the entering ligand, the range is 10^{-4} – 10^3 $\text{L mol}^{-1} \text{s}^{-1}$. Spectroscopic evidence shows that the intermediate has the same composition as the product; the metastable form is designated as $\text{MeReO}(\text{mtp})\text{Y}^*$. The structures of all the isolated products $\text{MeReO}(\text{mtp})\text{Y}$ have a single stereochemistry: Me and $-\text{SCH}_2$ lie in trans positions, as do Y and $-\text{SAr}$. This structure is believed to be reversed in the transient, Y and $-\text{SCH}_2$ occupying trans positions. Further support for this assignment comes from the ^{31}P splitting of the ^1H NMR spectrum, where additional coupling indicates unusual four-bond coupling from a W-pattern of the hydrogen and phosphorus atoms. The intermediate does not undergo an intramolecular rearrangement to the final product; instead, it reacts with a ligand of the same type in an intermolecular reaction leading to rearrangement. The activation parameters were determined for selected reactions, and the results support a mechanism with considerable associative character; ΔS^\ddagger values are ca. -125 $\text{J K}^{-1} \text{mol}^{-1}$. Because ligand Y must enter the coordination sphere from the vacant coordination position trans to the $\text{Re}=\text{O}$ group, a means must be devised for the leaving group X to gain that position. To account for the intervention of the isomer while honoring the principle of microscopic reversibility, two mechanisms are proposed. One involves a C_3 (“turnstile”) rotation of a specific group of three ligands in the six-coordinate transition state. Turnstile rotation of the groups X, Me, and Y can accomplish the needed transposition; the transition state passes through an approximate trigonal prismatic configuration, giving rise to a different and less stable isomer. The alternative mechanism, which may more easily accommodate data for $\text{Y} = \text{Me}_2\text{bpy}$, involves rearrangement of the common octahedral intermediate to a pentagonal pyramid. The arrangement of ligands in the intermediate, governed by their sizes, determines that isomerization accompanies product formation. Following either rearrangement, a second reaction, between $\text{MeReO}(\text{SCH}_2\text{C}_6\text{H}_4\text{S})\text{Y}^*$ and Y, then ensues by the *same* mechanism. The second rearrangement process then generates the more stable isomer of the product. Results are also presented from a study of monomerization of the dimeric rhenium species, $\{\text{MeReO}(\text{mtp})\}_2$, with phosphines(X) of various size and basicity. The results support a mechanism with two intermediates on the pathway to $\text{MeReO}(\text{mtp})\text{X}$.

Introduction

Oxorhenium compounds are known to catalyze oxygen-atom-transfer reactions between closed-shell molecules. Thus, as has been reviewed,^{1–3} MeReO_3 (MTO) catalyzes oxidations by hydrogen peroxide:



where $\text{X} = \text{R}_2\text{S}$,⁴ PR_3 ,⁵ alkenes,^{6,7} hydroxylamines,⁸ anilines,⁹ etc.¹ Also, the couple $\text{MeReO}_3/\text{MeReO}_2$ catalyzes the reduction

of oxoanions, including even perchlorate ions, in aqueous solution:^{10,11}



The chemistry of oxorhenium compounds has been developed

* To whom correspondence should be addressed. E-mail: espenson@iastate.edu.

- (1) Espenson, J. H. *Chem. Commun* **1999**, 479–488.
- (2) Herrmann, W. A.; Kühn, F. E. *Acc. Chem. Res.* **1997**, *30*, 169–180.
- (3) Gable, K. P. *Adv. Organomet. Chem.* **1997**, *41*, 127–161.
- (4) Vassell, K. A.; Espenson, J. H. *Inorg. Chem.* **1994**, *33*, 5491–5498.

(5) Abu-Omar, M. M.; Espenson, J. H. *J. Am. Chem. Soc.* **1995**, *117*, 272.

(6) Al-Ajlouni, A.; Espenson, J. H. *J. Am. Chem. Soc.* **1995**, *117*, 9243–9250.

(7) Al-Ajlouni, A.; Espenson, J. H. *J. Org. Chem.* **1996**, *61*, 3969–3976.

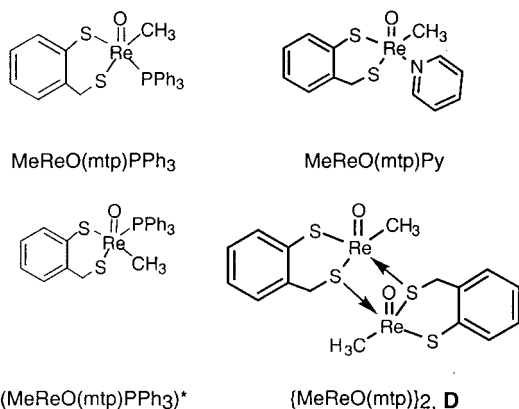
(8) Zauche, T. H.; Espenson, J. H. *Inorg. Chem.* **1997**, *36*, 5257–5261.

(9) Zhu, Z.; Espenson, J. H. *J. Org. Chem.* **1995**, *60*, 1326–1332.

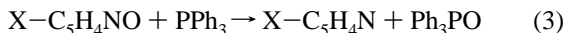
(10) Abu-Omar, M. M.; Espenson, J. H. *Inorg. Chem.* **1995**, *34*, 6239–6240.

(11) Abu-Omar, M. M.; Appleman, E. H.; Espenson, J. H. *Inorg. Chem.* **1996**, *35*, 7751–7757.

Chart 1



extensively in the past decade,^{2,12,13} as has that of their imido (R = NAr) relatives.¹⁴ The deoxygenation of pyridine *N*-oxides¹⁵ is catalyzed by the Re(V) compound MeReO(mtp)PPh₃ (Chart 1), eq 3, where mtpH₂ is 2-(mercaptomethyl)thiophenol. Many such compounds are now known and characterized, with L = phosphine, pyridine, thioether, and similar Lewis bases.^{16–18}



The success of these catalytic conversions rests on, among other factors, the replacement of an existing ligand by the substrate. At the very least, an assignment of a mechanism to O atom catalysis requires an understanding of ligand substitution. The MeReO(mtp)L compounds adopt an approximate square-pyramidal structure with the oxo group in the axial position; of those characterized to date, in every case the methyl group lies trans to the benzylic sulfur of mtp.^{16–18} This thermodynamic preference for a single stereoisomer proves to be an important feature of their substitution chemistry, as developed in the course of this research. We have undertaken studies of the following reaction:



Low-valent oxorhenium compounds have been shown to adopt an associative mechanism for ligand substitution,¹⁹ and the same appears true here. This system raises some important issues that, to our knowledge, have not been addressed before. Given the approximate square-pyramidal structure,²⁰ how can X and Y participate in a pathway that honors the principle of microscopic reversibility? This is rigorously required for exchange, X = Y, but can logically be extended to other pairs. Thus, if Y enters from the vacant lower axial position, then X

(12) Jung, J.-H.; Albright, T. A.; Hoffman, D. M.; Lee, T. R. *J. Chem. Soc., Dalton Trans.* **1999**, 4487–4494.

(13) Lahti, D. W.; Espenson, J. H. *Inorg. Chem.* **2000**, *39*, 2164–2167.

(14) McNeil, W. S.; DuMez, D. D.; Matano, Y.; Lovell, S.; Mayer, J. M. *Organometallics* **1999**, *18*, 3715–3727.

(15) Wang, Y.; Espenson, J. H. *Org. Lett.* **2000**, *2*, 3525–3526.

(16) Jacob, J.; Guzei, I. A.; Espenson, J. H. *Inorg. Chem.* **1999**, *38*, 1040–1041.

(17) Lente, G.; Guzei, I. A.; Espenson, J. H. *Inorg. Chem.* **2000**, *39*, 1311–1319.

(18) Lente, G.; Jacob, J.; Guzei, I. A.; Espenson, J. H. *Inorg. React. Mech. (Amsterdam)* **2000**, *2*, 169–177.

(19) Mayer, J. M.; Tulip, T. H.; Calabrese, J. C.; Valencia, E. *J. Am. Chem. Soc.* **1987**, *109*, 157–163.

(20) Concerning these descriptors: "...the difference between an 'approximate trigonal bipyramid' and an 'approximate square pyramid' may be vanishingly small." [Langford, C. H.; Gray, H. B. *Ligand Substitution Processes*; W. A. Benjamin, Inc.: New York, 1965; p 1918]. The second designation is used here in the interest of providing a pictorial frame of reference, not to exclude the alternative.

cannot leave from an equatorial position. Whether concerted or sequential, the reaction coordinate must be symmetric. One indication of the mechanistic complexity of reaction 4 is the finding that it proceeds by way of a characterizable intermediate of the same composition (by NMR) as MeReO(mtp)Y; it is a metastable isomer that we indicate with the designation MeReO(mtp)Y*.

The kinetic data are in accord with either of two mechanisms, both of which have as a first step the low-barrier, reversible, and unfavorable addition of Y to the vacant lower axial position. We consider two ways by which the resulting octahedral intermediate advances the reaction. First, there may be a trigonal rotation of the ligand set Me, X, and Y. This is a *turnstile* mechanism.^{21–25} As will be demonstrated, it brings the necessary symmetry to the mechanism by way of an approximately trigonal prismatic intermediate. Alternatively, the lower axial group may move into the equatorial plane to give a structure that, in the limit, is a pentagonal pyramid. Tests of these models will be presented. For specific reasons, these compounds adopt pathways for ligand substitution that are distinctly different from the norm: the five-coordinate reagents do not undergo labile rearrangement (i.e., they are not fluxional); remarkably, they add a sixth ligand. The resulting six-coordinate species rearrange unimolecularly through a prismatic or pentagonal intermediate before returning to the altered five-coordinate form. The rationale for these transformations has been explored.

Also bearing on mechanistic issues in catalysis, it should be noted that the dirhenium compound {MeReO(mtp)}₂ (D, Chart 1) reacts with the same set of ligands according to this *reversible* reaction:^{18,26}



It, too, starts with attack of L at either (sometimes both) of the equivalent, vacant axial sites. Some of the same issues are involved in the mechanism of monomerization, not the least of which are the question of the possible involvement of MeReO(mtp)Y* and an assessment of the extent to which any MeReO(mtp)Y is formed directly.

Experimental Section

Reagents. MTO was prepared from sodium perchrenate according to a published procedure.²⁷ The dimeric complex {MeReO(mtp)}₂ was prepared from MTO and mtpH₂ as previously reported.¹⁶ Mixing a 2.1:1 molar ratio of phosphine to dimer in toluene resulted in MeReO(mtp)-PR₃. The solvent was removed and the compound purified by recrystallization from methylene chloride–hexanes after cooling to –10 °C. This procedure was successful for the previously prepared compound with PPh₃, as well as for new compounds that are analogues of it, with PMePh₂, PCyPh₂, PPhCy₂, P(4-ClC₆H₄)₃, P(4-FC₆H₄)₃, and P(4-MeC₆H₄)₃.

Previously, MeReO(mtp)PR₃ complexes of PPh₃ and other phosphines were characterized spectroscopically and crystallographically.¹⁶ Each complex was characterized by ¹H NMR, ³¹P NMR, and UV/visible spectroscopy. One can see from Figure 1 that MeReO(mtp)PR₃

(21) Ramirez, F.; Ugi, I. *Adv. Phys. Org. Chem.* **1971**, *9*, 25–126.

(22) Gillespie, P.; Hoffman, P.; Klusacek, H.; Marquarding, D.; Pfohl, S.; Ramirez, F.; Tsolis, E. A.; Ugi, I. *Angew. Chem., Int. Ed. Engl.* **1971**, *10*, 687–715.

(23) Ugi, I.; Marquarding, D.; Klusacek, H.; Gillespie, P.; Ramirez, F. *Acc. Chem. Res.* **1971**, *4*, 288–296.

(24) Casares, J. A.; Espinet, P. *Inorg. Chem.* **1997**, *36*, 5428–5431.

(25) Casares, J. A.; Espinet, P.; Soulantica, K.; Pascual, I.; Orpen, A. G. *Inorg. Chem.* **1997**, *36*, 5251–5256.

(26) Jacob, J.; Lente, G.; Guzei, I. A.; Espenson, J. H. *Inorg. Chem.* **1999**, *38*, 3762–3763.

(27) Herrmann, W. A.; Kratzer, R. M.; Fischer, R. W. *Angew. Chem., Int. Ed. Engl.* **1997**, *36*, 2652–2654.

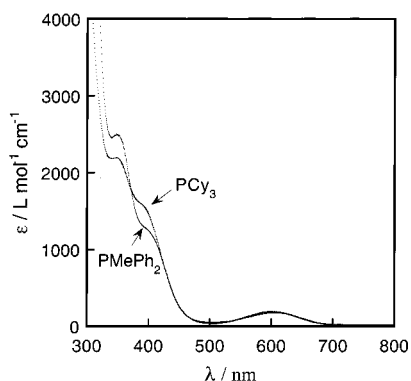


Figure 1. UV/visible spectra of two compounds MeReO(mtp)-PR₃, with PMePh₂ and PCy₃. The difference at 500–700 nm is too small to be useful, whereas that near 400 nm provided a precise measure of the reaction progress.

complexes are characterized by a weak absorption maximum near 600 nm ($\epsilon \approx 200 \text{ L mol}^{-1} \text{ cm}^{-1}$) and a much stronger shoulder near 400 nm ($\epsilon \approx 1500 \text{ L mol}^{-1} \text{ cm}^{-1}$). Extinction coefficients and NMR data are presented for numerous MeReO(mtp)PR₃ complexes in Tables S-1 and S-2 (Supporting Information). The difference in intensity between the 600 nm band of reactant and product is too low to be useful for kinetics. Thus, most studies were carried out in the vicinity of 400 nm.

The isolated MeReO(mtp)PR₃ complexes were used directly as the starting materials in the kinetics determinations. Because pyridine complexes coordinate more weakly than phosphines, an isolated MeReO(mtp)Py complex will dissociate to considerable extent, giving rise to an equilibrium proportion of the dimer as in eq 5. For that reason, the reactions of MeReO(mtp)Py complexes were carried out in the presence of added pyridine to prevent formation of {MeReO(mtp)}₂. It was shown that a ≤ 10 -fold increase in the concentration of free pyridine was immaterial. Benzene was used as the solvent for reaction kinetics.

Kinetics. A Bruker DRX-400 spectrometer was used to record NMR spectra. Chemical shifts were recorded relative to Me₄Si or the residual proton peak of the deuterated solvent. Shimadzu 3101 and 2501 spectrophotometers were used for optical spectra and to monitor reactions that lasted longer than ca. 30 s. Two stopped-flow (SF) instruments were used for more rapid reactions; one is a single-wavelength Applied Photophysics Laboratories (APL) instrument that was also used in sequential mixing experiments, the other an OLIS SF apparatus with a rapid-scanning monochromator and global fitting programs. The SF data obtained with the OLIS instrument were collected over a 230 nm range, usually 310–540 nm. That window was sometimes narrowed to 350–475 nm when little absorbance change could be detected outside that range. Ligand exchange reactions usually used the entering ligand at 1–40 mM, a much higher concentration than that of the starting complex, typically 80 μM . Reactions of MeReO(mtp)Py complexes also contained free pyridine at a concentration of about 1–5 mM. Because the formation constants are $K(\text{M}-\text{PR}_3) \gg K(\text{M}-\text{Py})$, these reactions proceeded to completion, and their rates were independent of the pyridine concentration over the range investigated. The data were analyzed by single-exponential (pseudo-first-order) or biexponential equations, as needed.

A sequential SF experiment with the APL instrument was carried out in which the two components, M-NC₅H₄Bu^t and PMePh₂, were mixed as usual. After a selected time (usually 3.0 s) in the “aging loop”, a final reagent (PMe₂Ph) was mixed automatically with the first two. Data from five replicates were averaged to obtain the final rate constant. Similar experiments with different reagents that allowed for a longer delay (ca. 120 s) were performed by rapidly introducing freshly prepared solutions into the OLIS instrument, such that the first measurement could be taken just at 120 s.

The two equations used for fitting most absorbance–time data are those for first-order kinetics, eq 6, and biexponential kinetics, eq 7, as

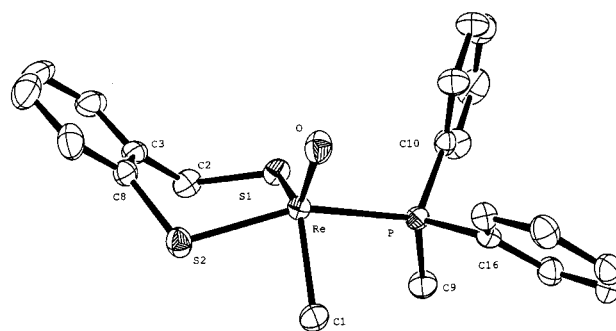


Figure 2. Perspective view of the molecular structure of MeReO(mtp)PMePh₂ with thermal ellipsoids at the 30% probability level. Selected bond lengths (pm) and angles (deg) are as follow: Re–O, 168.4(2); Re–C, 213.2(3); Re–P, 245.4(1); Re–S(1), 227.6(1); Re–S(2), 232.1(1); S(1)–C, 184.9(3); S(2)–C(8), 178.2(3); O–Re–C(2), 115.8(1); O–Re–S(1), 119.9(1); C(1)–Re–S(2), 123.7(1); O–Re–S(2), 106.5(1); S(1)–Re–S(2), 91.37(3), and C(1)–Re–S(2), 80.22(8). Additional structural parameters are given in Table S-5.

in the case where two pseudo-first-order reactions occur in sequence.

$$\text{Abs}_t = \text{Abs}_\infty + (\text{Abs}_0 - \text{Abs}_\infty) e^{-kt} \quad (6)$$

$$\text{Abs}_t = \text{Abs}_\infty + \alpha e^{-k_1 t} + \beta e^{-k_2 t} \quad (7)$$

Isolation and Crystallographic Studies. The compound MeReO(mtp)PMePh₂ was prepared from 30 mg of {MeReO(mtp)}₂ in benzene and 2.1 equiv of PMePh₂. The solution was allowed to evaporate over 2 d, giving bright green crystals in 80% yield. Elemental analysis: found C, 44.72 (calcd 44.12); H, 3.87 (3.88); S, 10.2 (11.2).

The crystal evaluation and data collection were performed on a Bruker CCD-1000 diffractometer with Mo K α ($\lambda = 0.71073 \text{ \AA}$) radiation. The distance from the diffractometer to the crystal was 5.08 cm. All non-hydrogen atoms were refined with anisotropic displacement coefficients. The hydrogen atoms were included in the structure factor calculation at idealized positions and were allowed to ride on the neighboring atoms with relative isotropic displacement coefficients. The software and sources of the scattering factors are contained in the SHELXTL program library, version 5.1.²⁸ The absorption correction was based on fitting a function to the empirical transmission surface as sampled by multiple equivalent measurements.²⁹

Results

X-ray Crystallography. Previously determined structures of MeReO(mtp)L complexes are those with L = PPh₃,²⁸ Py,¹⁷ 1,1,3,3-tetramethylthiourea,¹⁸ 4-acetylpyridine¹⁸ and 1,3-diethylthiourea.¹⁷ With that, further structural determinations might seem redundant, were it not for the way in which the mechanistic results of this study pointed toward an intermediate that might be an isomeric form, distinct from all of these. Thus, the structure of the compound MeReO(mtp)PMePh₂ was determined by single-crystal X-ray diffraction. The crystallographic information is summarized in Tables S-3 to S-7 in the Supporting Information. The molecular structure is depicted in Figure 2, with a few key bond distances and angles given in the caption. Complete information is given in Table S-5 and Figure S-1. This structure is analogous to the preceding ones. The groups about rhenium form an approximate square pyramid²⁰ with the oxo group at the apex. All four compounds adopt the same structural format: the CH₃ group is trans to the S atom attached to the benzylic carbon; the phenolic S lies trans to the Lewis base, here the P atom of PMePh₂. This arrangement was found

(28) Sheldrick, G. Bruker Analytical X-Ray Systems; Siemens: Madison, WI, 1997.

(29) Blessing, R. H. *Acta Crystallogr.* **1995**, *A51*, 33–38.

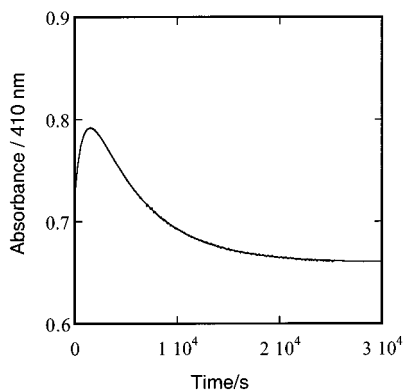


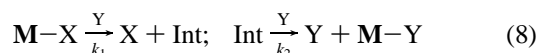
Figure 3. Absorbance–time data for a reaction between 0.58 mM MeReO(mtp)PPh₃ and 45 mM PCyPh₂ at 298 K in benzene. A fit to biexponential kinetics gave the following rate constants: $k_{\alpha} = 1.15 \times 10^{-3} \text{ s}^{-1}$ and $k_{\beta} = 1.83 \times 10^{-4} \text{ s}^{-1}$.

irrespective of the electronic and steric attributes of the coordinated ligand.

From these data we postulate, therefore, that all stable compounds of this family have analogous structures. That is to say, this structure is the thermodynamically preferred one for all phosphine and pyridine ligands. This argument is key to other assignments that we are making as to the probable structure of a metastable intermediate detected by kinetics and spectroscopy. We suggest that the intermediate has the CH₃ group and ligand reversed.

Initial Observations. We have examined reactions of the compounds MeReO(mtp)X, where X is used to represent the leaving ligand, phosphine (usually) or pyridine (occasionally), with an entering group Y, a different phosphine, to yield MeReO(mtp)Y. This seemingly simple transformation has proved to be more elaborate than this, however, and it affords new mechanistic insights. In many cases the kinetics and spectroscopy provided direct evidence for the intervention of an intermediate. In others, the intermediate could not be detected, but we will demonstrate that it is mostly likely disguised but not absent.

It is instructive first to examine one particular combination, X = PPh₃ and Y = PCyPh₂ (Cy = cyclohexyl). When followed spectrophotometrically with [Y] \gg [MeReO(mtp)X], the absorbance at 400 nm first rises and then falls (Figure 3). The same experiment monitored by ¹H NMR spectroscopy shows the buildup of a resonance at 5.1 ppm that later disappears. Analysis of the absorbance–time data, given the large excess of the entering ligand, was made by biexponential kinetics, which gave excellent fits at each set of concentration conditions. The pair of pseudo-first-order rate constants so determined are designated k_{α} and k_{β} , labeled so that $k_{\alpha} > k_{\beta}$. We defer momentarily a specification as to which rate constant applies to the first or second step in the chemical reaction scheme, for which the designations k_1 and k_2 are reserved. The kinetics determinations were carried out at several concentrations of PCyPh₂. Figure 4 shows that both k_{α} and k_{β} are linear functions of [Y] that extrapolate to the origin. Thus, both stages are displacement processes, not only the first. An abbreviated scheme is therefore



NMR spectroscopic data show that the intermediate contains M and Y, but not X, as written in eq 8. The doublet pattern for CH₃ in the ¹H NMR spectrum shows that M–X, M–Y, and

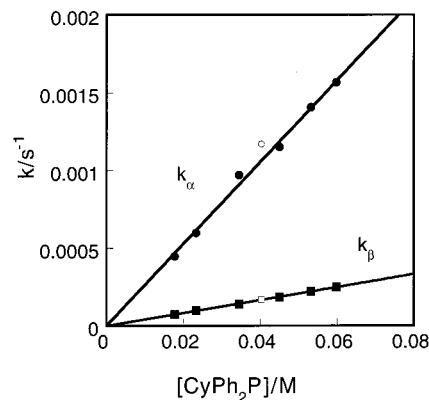


Figure 4. Plots showing values of k_{α} (circles) and k_{β} (squares) against [PCy₂Ph], including data taken at two wavelengths, 360 (filled symbols) and 410 nm (open symbols). The least-squares slopes are 2.4×10^{-2} and $4.2 \times 10^{-3} \text{ L mol}^{-1} \text{ s}^{-1}$.

the intermediate contain a single phosphorus atom coordinated to Re; a more complex splitting pattern would have been seen had both X and Y remained coordinated in the intermediate species.

Successive Displacement Reactions. The NMR pattern is the same for the other X,Y pairs whose reactions follow biexponential kinetics. For each ligand pair, it was possible to evaluate its two first-order rate constants and substantiate that each varies linearly with the concentration of Y. The resulting data take the form of second-order rate constants k_{α}^s and k_{β}^s , which are summarized in Table 1. Three entering ligands were used, Y = PCyPh₂, PCy₂Ph, and P(4-MeC₆H₄)₃. For each Y, one member of the pair of rate constants for a given X ligand has the same value, within the precision of resolving the pair of values from biexponential fitting. Irrespective of whether the constant member is a value of k_{α}^s or k_{β}^s , we designate it as k_2 . This assignment rests on the fact that the second-stage reaction does not retain any involvement of X (see eq 8). To reiterate this important point: according to eq 8, every reaction of a given Y has the second chemical step identical for all X ligands. Thus, the rate constant k_2 must be the same for each X ligand. The data in Table 1 show that constancy reasonably well and thus lend support to the reaction model. By default, the other second-order rate constant is k_1 . Of course, either k_1 or k_2 may be the larger number, depending on the chemical reagents; in contrast, $k_{\alpha}^s > k_{\beta}^s$, simply as a matter of definition.

NMR Studies of the Intermediate. The reaction between MeReO(mtp)PPh₃ and PCyPh₂ gave rise to a new resonance at 5.1 ppm that developed and then disappeared; see Figure S-2. Since its intensity is not large, it is clear that the intermediate never attains a high concentration. The spectrophotometric data afforded rate constants of 2.6×10^{-2} and $4.1 \times 10^{-3} \text{ L mol}^{-1} \text{ s}^{-1}$. The assignment made earlier, $k_2 = 2.6 \times 10^{-2} \text{ L mol}^{-1} \text{ s}^{-1}$, made on the basis that k_2 would be the same for all X, is thus confirmed. Only when the second rate constant is much larger than the first will the intermediate be held at a low concentration. From these values, the maximum extent of buildup of the intermediate is

$$\frac{[\text{Int}]_{\text{max}}}{[\text{MeReO(mtp)PPh}_3]_0} = \left(\frac{k_2}{k_1} \right)^{k_2/(k_1-k_2)} \quad (9)$$

which is 11% in this instance. This agrees with the value obtained from integration of the NMR spectra, ca. 10% intermediate at the maximum. The results of a similar reaction between MeReO(mtp)(4-ClC₆H₄)₃ and PCyPh₂ gave rise to 45%

Table 1. Rate Constants for the Biphasic Ligand Exchange Reactions between MeReO(mtp)X and Y (X, Y = Leaving, Entering Ligands)^a

entry	X	sorted by k_{α}^s and k_{β}^s (L mol ⁻¹ s ⁻¹)		sorted by k_1 and k_2 (L mol ⁻¹ s ⁻¹)	
Part A: Y = PCyPh ₂					
1	P(4-MeC ₆ H ₄) ₃	0.021	0.0016	0.0016	0.021
2	PPh ₃	0.026	0.0041	0.0041	0.026
3	P(4-FC ₆ H ₄) ₃	0.035	0.023	0.035	0.023
4	P(4-ClC ₆ H ₄) ₃	0.037	0.024	0.037	0.024
5	Cl ⁻	0.52	0.024	0.52	0.024
6	PMePh ₂ ^b	(~0.09)	(~0.05)		
Av: 0.024					
Part B: Y = PCy ₂ Ph					
7	P(4-MeC ₆ H ₄) ₃	2.7×10^{-4}	1.0×10^{-4}	1.0×10^{-4}	2.7×10^{-4}
8	PPh ₃	4.4×10^{-4}	1.9×10^{-4}	4.4×10^{-4}	1.9×10^{-4}
9	P(4-ClC ₆ H ₄) ₃	5.5×10^{-3}	2.5×10^{-4}	5.5×10^{-3}	2.5×10^{-4}
Av: 2.4×10^{-4}					
Part C: Y = P(4-MeC ₆ H ₄) ₃					
10	PMePh ₂ ^c	0.021	0.0016		
11	PPh ₃	0.048	0.0023	0.0023	0.048
12	P(4-ClC ₆ H ₄) ₃	0.055	0.033	0.033	0.055
Av: 0.051					

^a In benzene at 25 °C; the rate law in each step is directly proportional to [Y]; the second-order rate constants are from the fitting of k against [Y]. ^b Poor resolution by biexponential fitting. ^c The larger rate constant for this compound deviates from the established pattern by more than a factor of 2 for reasons that are not known.

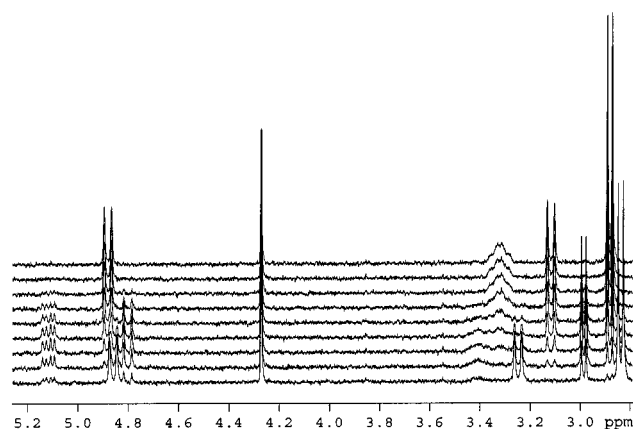


Figure 5. Stacked ¹H NMR spectra recorded during the reaction of 3.5 mM MeReO(mtp)P(4-ClC₆H₄)₃ and 36 mM PCyPh₂ in C₆D₆ at 25 °C. The peaks of the intermediate have resonances at 2.99 (CH₃-Re), 5.1, and ca. 4.9 (two CH₂ protons) ppm.

buildup of the intermediate observed, as depicted in Figure 5, in agreement with the calculation from eq 9, given the assignment of reaction steps in Table 1. Figures S-3 and S-4 show the time evolution of the intensities of each product, starting material, and intermediate attained by integration of the NMR experiments shown in Figures 5 and S-2, respectively. The NMR spectrum of the intermediate is quite distinct. The CH₃ resonance is split into a doublet by a single ³¹P from Y; X is absent in the spectrum of the intermediate, consistent with eq 8.

Reactions Showing Single-Stage Kinetics. Absorbance–time data from a number of other groups of reactions between MeReO(mtp)X and Y are accurately fit by simple first-order kinetics. With X = PPh₃ and Y = PMePh₂, for example, the time course for product buildup is defined with $k = 2.02 \times 10^{-3}$ s⁻¹ in benzene at 25.0 °C. Figure S-5 illustrates the data and the least-squares fitting. The occurrence of monophasic kinetics is not an isolated instance, as shown for the 10 entries in Table 2; in these cases, no intermediates were detected by NMR. Figure S-6 shows the linear relationship between the concentration of MePh₂P and the observed rate constant for its reaction with MeReO(mtp)PPh₃, with some NMR data included as well (Figure S-7).

Table 2. Rate Constants for the Monophasic Ligand Exchange Reactions between MeReO(mtp)X and Y (X, Y = Leaving, Entering Ligands)^a

entry	X	k/L mol ⁻¹ s ^{-1 b}
Y = PMePh ₂		
1	P(4-ClC ₆ H ₄) ₃	2.83(2)
2	P(4-FC ₆ H ₄) ₃	1.10(2)
3	PPh ₃	0.282(5)
4	P(4-MeC ₆ H ₄) ₃	0.089(1)
5	PCyPh ₂	0.062(1)
6	PCy ₂ Ph	0.0220(3)
7	PCy ₃	0.0018(1) ^c
Y = PMe ₂ Ph		
8	PPh ₃	23.0(1)
9	PMePh ₂	37(1)
Y = P(OMe)Ph ₂		
10	PPh ₃	0.126(3)

^a At 25.0 °C in benzene. ^b These are believed to be values of k_1 in eq 8 (see text). ^c Result from NMR experiments; others from UV/visible kinetics.

Rather than invoke a different reaction scheme for this set, we have explored the possibility that those cases following first-order kinetics reflect just one limit of the general two-stage scheme in eq 8, except that one step is much faster than the other. The limit cannot be obtained with $k_2 \ll k_1$, for then the value of k for each grouping in Table 2 would represent k_2 , and the same value, independent of the identity of X, would have been found. Consequently, the reduction of biexponential to first-order kinetics arises from the reverse inequality, $k_2 \gg k_1$. That is, the experiments would record the values of k_1 , a quantity varying with X and Y; the contribution of the k_2 reaction would have been lacking since that step was relatively much faster.

A Better Leaving Group. To pursue the issue just alluded to, we chose to use as the starting compound a complex with X = 4-Bu^cC₅H₄N. Earlier work¹⁷ has shown that pyridine complexes are much more labile than phosphines. Experiments were carried out on three MeReO(mtp)NC₅H₄R derivatives and two phosphines. Figures S-8 and S-9 show juxtaposed spectra for such an experiment and a single-wavelength kinetic trace extracted from these data, which shows biexponential kinetics, respectively. Table 3 summarizes these rate constants. The smaller values can be identified as belonging to the second stage;

Table 3. Rate Constants ($\pm \sim 5\%$) for Biphasic Reactions between MeReO(mtp)Pyridine Complexes and Phosphines

	$k_a = k_1$	$k_b = k_2^a$
Part A: Y = PMePh ₂		
C ₅ H ₅ N	1.94×10^3	52
4-Bu ^t C ₅ H ₄ N	1.09×10^3	52.8
4-MeOC ₅ H ₄ N	1.04×10^3	53
Part B: Y = PMe ₂ Ph		
C ₅ H ₅ N	$\sim 2 \times 10^5$	$\sim 1.4 \times 10^3$
4-Bu ^t C ₅ H ₄ N	8.3×10^4	1.1×10^3

^a k_2 refers to the reaction between MeReO(mtp)Y* and Y.

Table 4. Rate Constants and Activation Parameters for Selected Ligand Exchange Reactions

leaving ligand	entering ligand	$k_{298}/$ L mol ⁻¹ s ⁻¹	$\Delta H^\ddagger/$ kJ mol ⁻¹	$\Delta S^\ddagger/$ J K ⁻¹ mol ⁻¹
Part A: Stable Complexes				
Bu ^t C ₅ H ₄ N	PMe ₂ Ph	8.25×10^4	8.1 ± 0.9	-124 ± 3
Bu ^t C ₅ H ₄ N	PMePh ₂	1.09×10^3	17.7 ± 1.0	-127 ± 3
PPh ₃	PMe ₂ Ph	2.2×10^1	26.9 ± 0.5	-128 ± 2
PPh ₃	PCyPh ₂	4.1×10^{-3}	47.6 ± 2.0	-130 ± 4
Part B: Metastable Intermediates ^a				
PMe ₂ Ph*	PMe ₂ Ph	1.1×10^3	19.5 ± 0.7	-121 ± 3
PMePh ₂ *	PMePh ₂	5.3×10^1	18.2 ± 1.0	-151 ± 3
PCyPh ₂ *	PCyPh ₂	2.4×10^{-2}	25.5 ± 2.0	-189 ± 6

^a The one case in which the intermediate reacts with a ligand different from the coordinated one: MeReO(mtp)PMePh₂* and PMe₂Ph, $k = 1.78 \times 10^3$ L mol⁻¹ s⁻¹.

MeReO(mtp)Y* + Y has $k_2 = 53$ L mol⁻¹ s⁻¹ (Y = PMePh₂) and 1.1×10^3 L mol⁻¹ s⁻¹ (Y = PMe₂Ph).

The significance of these rate constants can be appreciated by reference to Table 2. In reactions with these phosphines as Y, only a single stage was seen. For reasons already stated, the derived rate constants are the values of k_1 in the range 0.0018–2.8 L mol⁻¹ s⁻¹ for Y = PMePh₂. Naturally, then, with $k_2 = 53$ L mol⁻¹ s⁻¹, the second stage is so much more rapid than the first that it went undetected. The same considerations apply to the case Y = PMe₂Ph, for which $k_2 = 1.1 \times 10^3$ L mol⁻¹ s⁻¹.

These data confirm that all the reactions investigated follow the same two-step scheme. Of the three cases with kinetics that do not conform to a two-stage reaction, the two dealt with in this section can be seen to simplify to first-order kinetics only because of inequalities in the rate constant values.

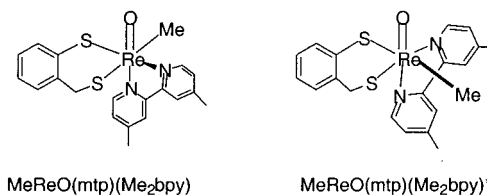
Diverting the Intermediate. The data have shown that the second reaction, between MeReO(mtp)Y* and Y, gives the final product MeReO(mtp)Y. The most reasonable interpretation of this finding is to suggest that this step is also a displacement of one Y by another. To demonstrate this, a system was found in which a third ligand Z could be introduced. For this purpose, MeReO(mtp)NC₅H₄Bu^t and PMePh₂ were first mixed in the stopped-flow apparatus. After a specified delay time of 3.0 s, calculated from the rate constants in Tables 4–6, so as to maximize the concentration of the intermediate, the third reagent, Z = PMe₂Ph, was introduced. The absorbance–time trace was then monitored at 390 nm. Scheme 1 depicts the reactions. Analysis of the kinetic data for this stage shows that the apparent first-order rate constant is directly proportional to [PMe₂Ph], as shown in Figure S-10. The rate constant for MeReO(mtp)-PMePh₂* and PMe₂Ph is 1.7×10^3 L mol⁻¹ s⁻¹. The slower stage in the kinetics originates from the independently known reaction of MeReO(mtp)PMePh₂ with PMe₂Ph. This is, incidentally, the single example in this work of a reaction in which the entering ligand is different from the ligand in the intermediate.

Table 5. Rate Constants for Monomerization of {MeReO(mtp)}₂ by Phosphines

PR ₃	$k_a/$ L mol ⁻¹ s ⁻¹	$k_b/$ L ² mol ⁻² s ⁻¹	$-\Delta H_{IP}/$ kcal mol ⁻¹	cone angle/deg	k_b/k_a
P(OMe) ₂ Ph	12.4(3)	ca. 0		120	0
PPh ₃ ^a	0.0082	0.052	21.2	145	6.4
PCy ₂ Ph	0.029	1.7(3)		164	58
PCyPh ₂	0.060(4)	6.2(4)		153	103
PCy ₃	0.13(4)	15(2)	33.2	170	115
PMePh ₂	3.5(6)	2100(150)	24.7	136	600
P(OMe)Ph ₂	$\sim 0.7(2)$	590(40)		132	842

^a From ref 17.

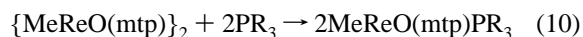
A second experiment explicitly for the intermediate was carried out between MeReO(mtp)NC₅H₄-4-Bu^t and Me₂bpy (4,4'-dimethyl-2,2'-bipyridine). Pyridine complexes exist in an approximately 9:1 ratio of isomers, favoring M–L over M–L*, unlike phosphine complexes, for which the M–L* isomer remains below the detection limit at equilibrium. This reaction gave two isomers:



Our characterization of the two reagents and two products can be made from the ¹H NMR spectra on the basis of their chemical shifts, as calibrated by similar isomers with monodentate phosphine ligands. The two methylene protons of the mtp ligand appear as two doublets, the separation between which is indicative of the isomer obtained. On the basis of such comparisons, we can readily suggest the structural assignments given.

Activation Parameters. Several biphasic reactions were recorded as a function of temperature. Biexponential fitting was used to resolve the two components. The resulting first-order rate constants were divided by the concentration of the entering reagents, generating the values of the rate constants for the first and second stages, k_1 and k_2 . The temperature dependence of each of these rate constants was analyzed in terms of the transition state theory equation, resulting in values of the entropy and enthalpy of activation. Thus, two sets of parameters result, one for the reaction of the stable stereoisomer, MeReO(mtp)X, and the other for the metastable form, MeReO(mtp)Y*. The results are presented in Table 4 (also Figure S-11).

Monomerization. An extensive set of data has been obtained pertaining to the rate of the following reactions:¹⁷



The rate law found from earlier work and confirmed for additional phosphines in this study is

$$\frac{d[\text{MeReO(mtp)PR}_3]}{dt} = \frac{[\{\text{MeReO(mtp)}\}_2](k_a[\text{PR}_3] + k_b\{\text{PR}_3\}^2)}{\quad} \quad (11)$$

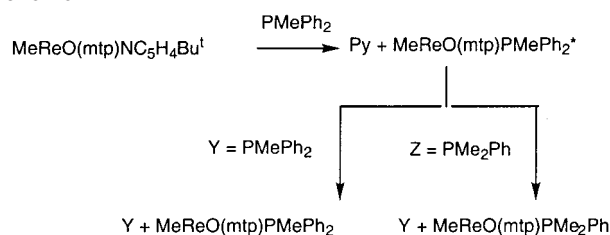
Table 5 presents the new data along with information from the earlier study. Figure S-12 shows the relationship between k and [CyPh₂P] for the monomerization reaction. To a rough approximation, the first-order phosphine pathway is adopted preferentially by phosphines of smaller size (cone angle), and

Table 6. Rate Constants^a as a Function of Leaving (X) and Entering (Y) Groups

Part A: MeReO(mtp)X + Y						
X	Y					
	PMe ₂ Ph	PMePh ₂	P(OMe)Ph ₂	PCyPh ₂	PCy ₂ Ph	P(4-MeC ₆ H ₄) ₃
Cl ⁻				0.52		
PMePh ₂	37.0			~0.09		0.0016
P(4-ClC ₆ H ₄) ₃		2.83		0.037	0.0055	0.033
P(4-FC ₆ H ₄) ₃		1.10		0.035		
PPh ₃	23.0	0.282	0.126	0.0041	0.00044	0.0023
P(4-MeC ₆ H ₄) ₃		0.089				
PCyPh ₂		0.062				
PCy ₂ Ph		0.0220				
PCy ₃		0.0018				

Part B: MeReO(mtp)Y* + Y					
X	Y				
	PMe ₂ Ph	PMePh ₂	PCyPh ₂	PCy ₂ Ph	P(4-MeC ₆ H ₄) ₃
MeReO(mtp)Y*	1100	53	0.024	0.0002	0.05

^a In benzene at 25 °C, in units L mol⁻¹ s⁻¹.

Scheme 1

vice versa. The situation is not straightforward, however: note that P(OMe)₂Ph, for which k_a carries the entire reaction, lies at one end of the selectivity range, whereas P(OMe)Ph₂ lies at the other. We calculated the relative importance of each pathway as a function of phosphine complexes for several PR₃ ligands (Figure S-13). Poorly donating PPh₃ primarily reacts through the first-order pathway.

For certain Y, the dimer gave some (M–Y)* along with (M–Y), especially for those ligands with a slower M–Y* + Y reaction. With PMePh₂ and PMe₂Ph, M–Y* could not be detected by ¹H NMR. Larger ligands gave initial yields of the M–Y* intermediate of 18% (PCyPh₂) and 25% (PCy₂Ph). Further studies are needed, however, as these data are quite limited.

Discussion

Experimental Findings. A succinct recapitulation of the experimental observations is given to guide the discussion. The reaction between MeReO(mtp)X (M–X) and Y gives the eventual product M–Y; both compounds have the same geometry. These reactions often follow biexponential kinetics. In the first stage, M–X and Y form an intermediate, M–Y*, with the same composition as M–Y. Both intermediate and product have a 1:1 ratio of Re:Y, and X is absent. In the second stage, M–Y* reacts with a *second* Y to form the stable product M–Y. The rate of each step in the sequence is also directly proportional to the concentration of Y. The rate constant for the second stage (between M–Y* and Y) is independent of the identity of X in the parent complex. A certain subset of the M–X + Y reactions seems to occur in a single stage, but that was shown to be a consequence of the inequality $k_2 \gg k_1$. With Py as the leaving group and Y the same, the first stage was much faster; again following biexponential kinetics. The rate constant of the slower stage is the value of k_2 for the reaction of M–Y* and Y, previously disguised. The values of both k_1

and k_2 depend on the identities of the leaving and entering ligands.

Issues of Mechanism. As to the molecular mechanism, this system poses some intricate questions that go beyond the reaction scheme presented in eq 8. A complete mechanism must, at the very least, account for the need for a two-stage mechanism, accommodate the precepts of microscopic reversibility, address the existence of an intermediate that can be detected and trapped, account for the trends in reactivity of each step in the mechanism, and satisfy the requirement for chemically reasonable species along the reaction coordinate.

The Intermediate Is an Isomer. The spectroscopic data point to M–Y* being an isomer of the stable M–Y; the suggested structural formula is given in Chart 1. When Y is a phosphine, both M–Y* and M–Y complexes show a doublet resonance in the ¹H spectrum for the CH₃Re group from splitting by ³¹P. The ³¹P NMR spectrum reveals that both peaks of both forms have similar but recognizably different chemical shifts. This shows that only one phosphorus atom is coordinated because a more complex splitting pattern is found with Y = 1,2-bis-(diphenylphosphino)benzene. Its chelating phosphorus atoms are inequivalent, and a complex family of multiplets results.

The inequivalent methylene protons of mtp appear as doublets with $J \approx 12$ Hz, from coupling between the diastereotopic hydrogens. Both methylene resonances in the M–Y* species lie downfield of those in M–Y. The separation between the doublets in M–Y* is 0.2–0.75 ppm, compared to 1.1–1.7 ppm in M–Y. Once established, this pattern can serve as a diagnostic tool of structure in compounds for which the assignment is less evident.

In every instance in which the ¹H NMR spectrum of M–Y* (here, Y has a P donor atom) could be recorded, a further splitting of one (but not both) of the methylene protons of mtp in the ¹H NMR spectrum was found, making it appear as a doublet of doublets. The secondary coupling has a J of about 4.5 Hz. The secondary splitting was absent, however, for the more stable isomer, which shows both protons as simple doublets:

chemical shifts for CH ₂	MeReO(mtp)L	MeReO(mtp)L*
L = PCyPh ₂	4.90 (d), 3.13 (dd)	5.10 (d), 4.80 (d)
L = PCy ₂ Ph	5.05 (d), 3.39 (dd)	5.16 (d), 4.68 (d)
L = 4-Bu ^c C ₅ H ₄ N	4.79 (d), 3.78 (dd)	5.21 (d), 4.89 (d)
L = Me ₂ bpy	5.27 (d), 4.15 (d)	5.45 (d), 4.72 (d)

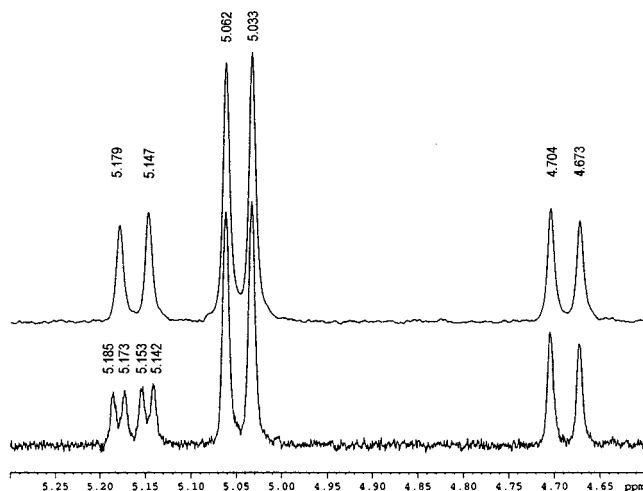
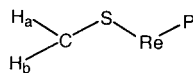


Figure 6. ^1H and $^1\text{H}\{^{31}\text{P}\}$ NMR spectra of a solution containing both isomers of $\text{MeReO}(\text{mtp})\text{PCy}_2\text{Ph}$ over a narrow range of chemical shifts. The doublet at 5.04 ppm is from one of the methylene protons of the more stable isomer. The other resonances arise from the pair of methylene protons of $\text{MeReO}(\text{mtp})\text{PCy}_2\text{Ph}^*$. The downfield resonance appears as a doublet of doublets owing to four-bond coupling to ^{31}P ; that resonance becomes a doublet as well upon broadband decoupling.

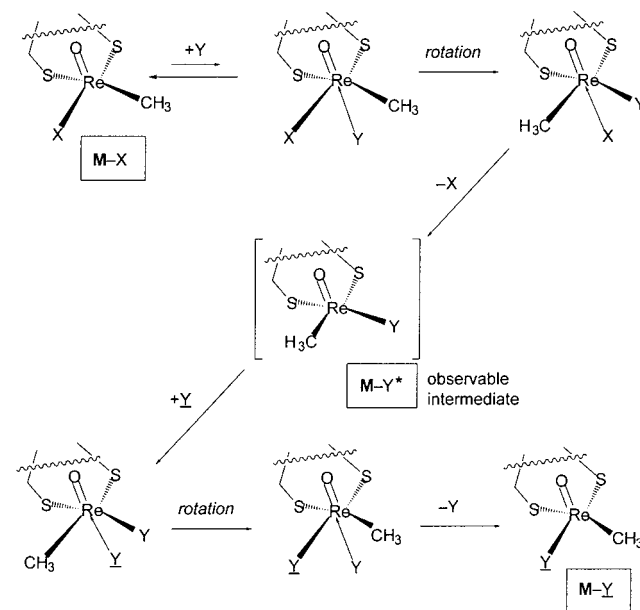
Broadband decoupling of ^{31}P centered at 25 ppm removed the secondary splitting; it is thus shown to arise from a coupling to ^{31}P . The original and decoupled spectra are presented in Figure 6. That the secondary splitting should occur in the isomer having the methylene group bonded to the S trans to P, but not in that with a cis arrangement, suggests to us an unusual four-bond coupling pattern. A few precedents in organic compounds can be cited.^{30–32} Further, a coupling pattern not dissimilar to that seen in these experiments was observed for one H atom of a metal-coordinated SH_2 ; one H appears as a doublet of doublets (the first coupling from diastereotopic hydrogens) owing to an ancillary phosphine ligand that is also coordinated to the metal.³³

Long-range (four-bond) couplings may occur when a W-configuration exists. Such an arrangement can be drawn here, involving $\text{H}_a\text{H}_b\text{-C-S-Re-P}$. Its two three-atom components form a dihedral angle of ca. 160° ; planarity is not a requirement, however. This is the arrangement of atoms by which H_a couples to phosphorus:



The Reaction Mechanism. To account for the various issues raised, we suggest two variants for the mechanism. Both of them start with attack of the entering nucleophile on rhenium at the only reasonably available site, the open coordination position trans to the oxo group. This yields an intermediate with a six-coordinate, approximately octahedral structure. The interaction between Re and Y in this position must be weak, because monodentate ligands are not known to form six-coordinate structures in this group of compounds. It can be presumed that Y repeatedly enters and leaves prior to the next step; the initial step does not pose a significant kinetic barrier. The six-coordinate intermediate lies on the pathway for substitution; it must be transformed into a substance in which Y becomes strongly attached to rhenium as the bond to X weakens.

Scheme 2. Proposed Turnstile Mechanism



(a) A Turnstile Mechanism. Imagine that this is accomplished by a rotation about one particular pseudo- C_3 axis of the octahedron; this axis has the donor atoms of X and Y and the CH_3 group. This is termed a *turnstile* rotation. At a rotation angle of ca. 60° , the molecule passes through an approximately trigonal prismatic geometry. This is not unreasonable, because trigonal prismatic geometry is not too badly destabilized by the d^2 electronic configuration of $\text{Re}(\text{V})$. Instances of this geometry have been well established, including several rhenium compounds.^{34–37} This sequence is depicted in Scheme 2.

As rotation continues to ca. 120° , an approximately octahedral configuration is restored, which may take any of three forms. Trivially, the rotation would restore X, Y, and CH_3 to their original forms, and no net change would be realized. A second nonproductive event would be to place the CH_3 group trans to oxo; the strong Re-C covalent bond will not break, so further rotation presumably ensues. The rotation that puts X in the position trans to the oxo group gives the important intermediate that lies along the reaction coordinate. X then leaves from that position. It is the one at which Y entered; this premise satisfies microscopic reversibility.

The species so formed has the composition $\text{MeReO}(\text{mtp})\text{-Y}^*$; the asterisk denotes it as the detectable intermediate. Examination of the structural formulas in Scheme 2 reveals that turnstile rotation indeed produces a stereoisomer that is different from the stable form. Because $\text{MeReO}(\text{mtp})\text{Y}^*$ is not the stable form, as judged by crystal structures of various isolated complexes, it must undergo further rearrangement. This is accomplished not by a unimolecular process, but by a bimolecular one. A second entering ligand Y attacks the intermediate, as required by the form of the rate law.

It is only logical to presume that the second stage reaction adopts the same mechanism as the first. Following the structural formulas in Scheme 2, it can easily be seen that the same

(30) Cremer, S. E.; Chorvat, R. J. *J. Org. Chem.* **1967**, *32*, 4066.

(31) Griffin, C. E.; Kundu, S. K. *J. Org. Chem.* **1969**, *34*, 1532.

(32) Ross, J. A.; Martz, M. D. *J. Org. Chem.* **1969**, *34*, 399–404.

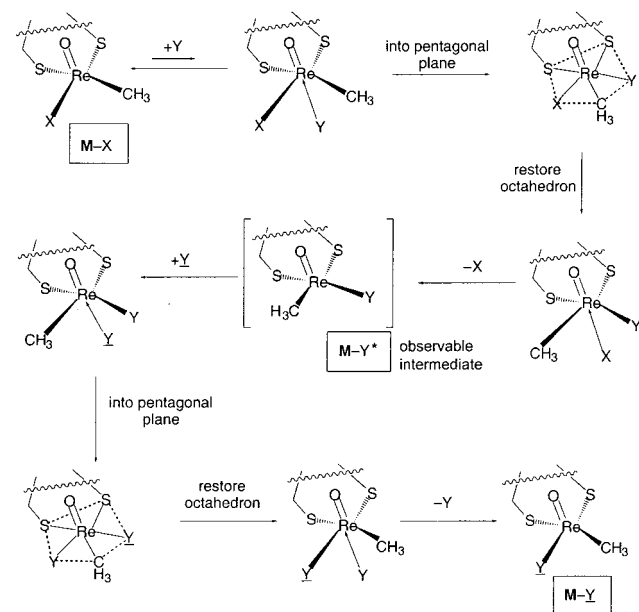
(33) Ma, E. S. F.; Rettig, S. J.; James, B. R. *Chem. Commun.* **1999**, 2463–2464.

(34) Blower, P. J.; Dilworth, J. R.; Hutchinson, J. P.; Nicholson, T.; Zubietta, J. J. *J. Chem. Soc., Dalton Trans.* **1986**, 1339–1345.

(35) Eisenberg, R.; Gray, H. B. *Inorg. Chem.* **1967**, *6*, 1844–1849.

(36) Stiefel, E. I.; Eisenberg, R.; Rosenberg, R. C.; Gray, H. B. *J. Am. Chem. Soc.* **1966**, *88*, 2956.

(37) Danopoulos, A. A.; Wong, A. A. C.; Wilkinson, G.; Hursthouse, M. B.; Hussain, B. *J. Chem. Soc., Dalton Trans.* **1990**, 315–331.

Scheme 3. Proposed Pyramidal Mechanism

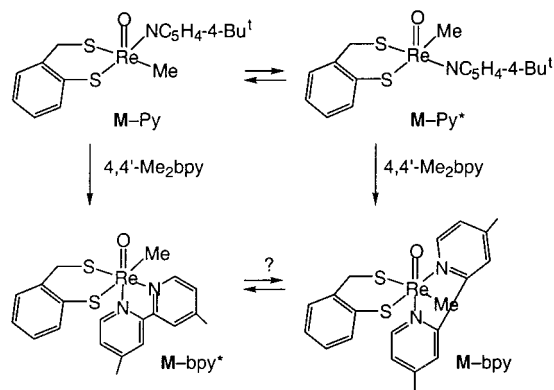
sequence of events produces the more stable isomer of $MeReO(mtp)Y$.

(b) A Pyramidal Mechanism. In this mechanism it is also proposed that ligand Y enters the coordination shell from the lower axial position to give an intermediate in which rhenium is six-coordinate with an approximately octahedral geometry. An intermediate with a pentagonal pyramidal structure would be formed if entering ligand Y of the octahedron moves into the equatorial plane, generating a second intermediate of the same composition but with an approximate pentagonal pyramidal geometry. Moreover, the significant steric demand of the phosphine (especially) and pyridine ligands indicates that only one position in the pentagonal plane is likely to be the site for entry of Y, that between the methyl group and the phenolic sulfur, to avoid close contact between the much larger ligands X and Y. Following that, or concurrent with it, one ligand X assumes the coordination position trans to the oxo group. If Y moves, no net reaction would be found; if X, the reaction is then completed to yield $M-Y^*$. When this metastable intermediate repeats the same steps with a second Y, the more stable $M-Y$ is obtained. The sequence of steps, which satisfies microscopic reversibility, is shown in Scheme 3.

Rather than this description, in which Y enters and then X moves, X and Y may move in concert to some extent so as to avoid one another. That would still lead to the $M-Y^*$ isomer, without passing through a fully formed pentagonal intermediate. This minor change can be kept in mind, but for simplicity in description it will not be emphasized.

Rearrangement from octahedral to pentagonal geometry, with the accompanying steric crowding, would be the only step with a significant kinetic barrier. Its reverse should be much more rapid, in that the strain is relieved. The two other steps entail addition or removal of a ligand to or from the weakly coordinating site trans to the oxo group and would not pose a significant barrier in rate (but perhaps in equilibrium, since the six-coordinate structure is less stable than the five-coordinate one).

From that argument, $k_{exp} = K_{56}k_{rearr}$, where K_{56} represents the equilibrium constant for axial addition of Y; $K_{56} \ll 1$, and k_{rearr} designates the rate constant for movement of a ligand into the equatorial plane. No NMR signal has been detected for any

Scheme 4. Reactions Forming Isomeric Bipyridine Complexes

six-coordinate form, $MeReO(mtp)L_2$. So, conservatively, $K_{56} < 10^{-2}$. On the other hand, as shown next, one can "force" formation of that form through the use of a bidentate ligand with a substantial chelate effect.

The differences between the turnstile and pentagonal mechanisms is not great and largely resides in the structure of the intermediate. As mentioned in the next sections, however, the pentagonal intermediate seems to account more readily for the observations when Y is a symmetric chelating ligand. A theoretical analysis of intramolecular rearrangements in six-coordinate complexes has recently been reported.³⁸ Data referring both to an associative mechanism for substitution and to the requirements of microscopic reversibility in reactions of related imidorhenium(V) have been presented and ably analyzed.¹⁴

Six-Coordination. In view of the proposal that Y adds to the vacant position trans to the oxo group, it is important to learn whether stable compounds exist with a six-coordinate geometry. Only when the chelate effect is invoked were such compounds obtained. In addition to the data reported here, examples of six-coordinate $MeReO(mtp)(LL)$ compounds are known with 1,2-bis(diphenylphosphino)benzene³⁹ and with bipyridine ligands such as Me_2bpy in this work and various other bpy and phen ligands.⁴⁰

The presumably concurrent reactions of Me_2bpy were carried out with a mixture of the isomers $MeReO(mtp)NC_5H_4-4-Bu^t$ and $MeReO(mtp)NC_5H_4Bu^t$ that remain in equilibrium. These isomers equilibrate fairly rapidly;⁴¹ the 1H NMR spectra show an equilibrium proportion of about 10% of the less favored isomer. From the pattern of chemical shifts (Table S-8), two products were identified, $MeReO(mtp)(Me_2bpy)^*$ (90%) and $MeReO(mtp)(Me_2bpy)$ (10%), as in Scheme 4.

Because the two pyridine compounds equilibrate within $t < 1$ min, both reactions with Me_2bpy have nearly the same rate constant, such that the product distribution reflects that of the parents. We ask if this is reasonable, because PMe_2Ph reacts differently with $MeReO(mtp)PMePh_2^*$ ($k = 1.7 \times 10^3 L mol^{-1} s^{-1}$) and $MeReO(mtp)PMePh_2$ ($k = 37 L mol^{-1} s^{-1}$). In defense of the original precept for pyridine ligands, however, it should be noted that all equilibrated complexes of the phosphine ligands give rise to an undetectably low concentration of the less stable isomer. Thus, reactions of the isomeric phosphine complexes proceed with substantially different driving forces, a factor that

(38) Soubra, C.; Oishi, Y.; Albright, T. A.; Fujimoto, H. *Inorg. Chem.* **2001**, *40*, 620–627.

(39) Saha, B.; Espenson, J. H., unpublished observations.

(40) Rockey, T. R.; Espenson, J. H., unpublished results.

(41) Shan, X.; Espenson, J. H., unpublished results.

may account for the kinetic advantage of one isomer. The pyridine complexes, on the other hand, differ in stability by only $\Delta G^\circ \approx 5 \text{ kJ mol}^{-1}$ in favor of M-Py , and the two isomers thus might differ little in reactivity.

A counter-argument can be offered, however, that the chelated bpy products come to equilibrium on their own. In that case, the product ratio would simply reflect the 9:1 equilibrium ratio of the MeReO(mtp)bpy isomers. That suggestion is untenable, however, because the less stable isomer is in the large majority. Under these conditions, no evidence was obtained for unimolecular isomerization of $\text{MeReO(mtp)(Me}_2\text{bpy)}$. The reaction in Scheme 4 with an arrow marked “?” does not occur, according to this interpretation. The cis–trans isomerization of $\text{Me}_2\text{ReO-(bpy)Cl}^{12}$ perhaps adopts a turnstile mechanism as well, contrary to the suggested mechanism in which one arm of the bpy chelate was proposed to dissociate.

The results for the Me_2bpy complex may be telling. From either isomer, one should be able to access the trigonal prismatic structure of the turnstile mechanism, which does not happen. On the other hand, a pentagonal intermediate is not possible, given the ligand structure and the premise of the mechanism. Assuming the turnstile mechanism is not precluded for some other reason, this logic leads one to prefer the mechanism with the pentagonal pyramidal intermediate.

The Rate Constants and Their Activation Parameters. The mechanism is associative, as shown by the first-order dependence on ligand Y in a step that gives rise to a six-coordinate intermediate in a fast prior equilibrium. The rate-controlling step is a major rearrangement, either the turnstile rotation or rearrangement to a pentagonal pyramid. To show the effects of changing X and Y, the rate constants for selected reactions are presented in a different arrangement in Table 6. The best Lewis bases are the most reactive nucleophiles Y; their influence is substantial, as represented both by the strength of the equilibrium interaction and by the increase in bonding strength as the stronger ligand Y turns into an equatorial position. The leaving group X has the opposite effect, the weakest nucleophiles reacting more rapidly. For X, however, the effect should be confined to the rearrangement step, as X moves into the lower axial position at which its bonding is weaker. Again, however, the overall chemistry is associative. This description describes the conversion of M-X to M-Y^* ; the second stage merely repeats the steps in the first.

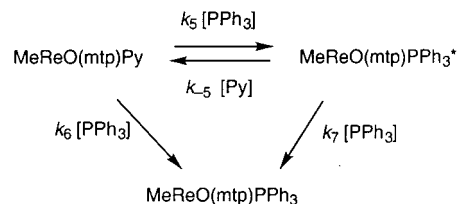
An interesting correlation of the kinetic data has been realized against the stereoelectronic parameter χ_d parameter from the QALE method for phosphine ligands.⁴² This parameter is a good measure of bonding ability. For a series of reactions in which the entering ligand Y was PMePh_2 , a linear plot of $\log k$ vs χ_d was obtained. Linear regression gives a slope of 0.19 ± 0.02 (Figure S-14). The same data show that bonding ability (measured by the $\text{p}K_a$ of R_3PH^+) and steric considerations (from the cone angle θ) both play a role. With these parameters, the correlation of the rate constant is given by $\chi_d = 27.79 - 1.47\text{p}K_a - 0.069\theta$. A Hammett LFER correlation yields $\rho = 1.3$ (Figure S-15), suggesting that negative charge builds up in the transition state.

$\text{MeReO(mtp)Py} + \text{PPh}_3$, a Reinterpretation. The rate of replacement of Py by PPh_3 from MeReO(mtp)Py was previously reported to occur by parallel pathways, one involving MeReO(mtp)PPh_3^* , the other “direct”, represented by the rate constant k_6 .¹⁷ The reaction sequence is shown in Scheme 5.

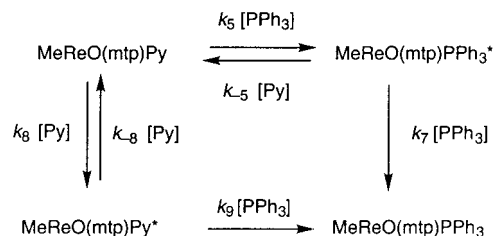
This model fits the data, with the following values of k/L

(42) Dias, P. B.; Minas de Piedade, M. E.; Martinho Simoes, J. A. *Coord. Chem. Rev.* **1994**, *135*, 737–807.

Scheme 5. Originally Proposed Route from Pyridine to Phosphine Complex



Scheme 6. Revised Reactions for Converting a Pyridine to a Phosphine Complex



$\text{mol}^{-1} \text{ s}^{-1}$: $k_5 = 88.0$, $k_{-5} = 16.1$, $k_6 = 6.27$, and $k_7 = 0.2$. Given these rate constants and the concentrations used, $k_{-5}[\text{Py}] \gg k_6[\text{PPh}_3]$; thus, the rate expression is

$$v = \left\{ k_6 + \frac{k_5 k_7 [\text{PPh}_3]}{k_{-5} [\text{Py}]} \right\} [\text{MeReO(mtp)Py}] [\text{PPh}_3] \quad (12)$$

We now propose an alternative in which both pathways proceed by way of the M-Y^* intermediate, and we now claim that a direct pathway does not exist. The new reactions are shown in Scheme 6.

Provided that $k_{-5}[\text{Py}] \gg k_6[\text{PPh}_3]$ and $k_{-8}[\text{Py}] \gg k_9[\text{PPh}_3]$ (both of which are valid assumptions since Py substitutions are so much faster than those of phosphines), the rate equation would be

$$v = \left\{ \frac{k_8 k_9}{k_{-8}} + \frac{k_5 k_7 [\text{PPh}_3]}{k_{-5} [\text{Py}]} \right\} [\text{MeReO(mtp)Py}] [\text{PPh}_3] \quad (13)$$

Because the two isomers exist in a 9:1 equilibrium ratio, $k_8/k_{-8} = 0.1$. When the leading term was thought to be the value of k_6 , its value was given as $6.27 \text{ L mol}^{-1} \text{ s}^{-1}$. With these values we arrive at $k_9 = 63 \text{ L mol}^{-1} \text{ s}^{-1}$. This is quite comparable to the value of k_5 ; both rate constants represent the displacement of a pyridine complex with triphenylphosphine, and it is not unreasonable that they would be similar in value.

Recall from earlier that the most reasonable interpretation of the 90:10 product ratio of the $\text{MeReO(mtp)(Me}_2\text{bpy)}$ isomers was that the two pyridine isomers had the same reactivity. Our supposition that $\text{MeReO(mtp)NC}_5\text{H}_4\text{Bu}^*$ and $\text{MeReO(mtp)NC}_5\text{H}_4\text{Bu}$ react with Me_2bpy at about the same rate is validated by reanalysis of the data given in the immediately preceding paragraphs.

Summary. A substantial family of the compounds MeReO(mtp)X ($X = \text{pyridine, phosphine}$) react with phosphines (Y) in two stages, via a reaction scheme in which an intermediate can be detected. It is a stereoisomer of the product. Rearrangement then occurs, and turnstile and pentagonal mechanisms have been proposed for each stage. Rearrangement accounts for isomer formation at each stage, while allowing for the principle of microscopic reversibility to be observed.

It is worth noting that the substitution pattern in this system reverses the usual case: the six-coordinate intermediate under-

goes rearrangement, whereas the five-coordinate form cannot. The prohibition seems to trace to the presence of the oxorhenium group, which would form a trigonal pyramid only with a prohibitive activation barrier.

Acknowledgment. This research was supported by the U.S. Department of Energy, Office of Basic Energy Sciences, Division of Chemical Sciences, under Contract W-7405-Eng-82. The crystallographic analysis was done by Dr. Ilia Guzei. Helpful conversations with Prof. J. G. Verkade, Prof. L. K. Woo, Gábor Lente, Xiaopeng Shan, and Oleg Pestovsky are gratefully acknowledged. Comments from a reviewer were helpful in formulating the pentagonal mechanism.

Note added in proof: Equilibrium constants from NMR studies were obtained at 25 °C for the overall reactions

$\text{MeReO(mtp)X} + \text{Y} \rightleftharpoons \text{MeReO(mtp)Y} + \text{X}$ for these (X, Y) pairs: (PPh₃, PMePh₂) 90(3); (PPh₃, PCyPh₂) 10(1); (PPh₃, P(4-MeC₆H₄)₃) 6.0(5); (PPh₃, PCy₂Ph) 5; (PCyPh₂, PCy₂Ph) 0.82; (PMePh₂, PCy₂Ph) 0.19; (PPh₃, P(4-ClC₆H₄)₃) 0.10; (P(4-MeC₆H₄)₃, P(4-ClC₆H₄)₃) 0.02.

Supporting Information Available: Complete tables of crystal data and refinement details, atomic coordinates, bond lengths and angles, and anisotropic displacement parameters; spectroscopic information, and graphs and plots of kinetic data (PDF). This material is available free of charge via the Internet at <http://pubs.acs.org>.

JA004145H